

Chiral Recognition Among Tris(diimine)–Metal Complexes, 6^[‡]

Racemic Compound Formation *versus* Conglomerate Formation with [M(bpy)₃](PF₆)₂ (M = Ni, Zn, Ru); Molecular and Crystal Structures

Josef Breu,^{*,[a]} Holger Domel,^[a] and Alexander Stoll^[a]

Keywords: Molecular recognition / Chiral recognition / Conglomerate crystallization / Self-assembly / Polymorphism

Minor modifications in molecular size and shape induced by variation of the central atom drastically alter the crystallization behaviour of the hexafluorophosphate salts of [M(bpy)₃]²⁺. With M = Ru, racemic solutions crystallize as true racemates in the β -type [$P\bar{3}c1$, $a = 10.6453(5)$, $c = 16.2987(9)$ Å, $Z = 2$], while for M = Zn the racemic structure cannot be obtained, as spontaneous resolution [γ -type [$P3_1$, $a = 10.3873(5)$, $c = 26.1309(16)$ Å, $Z = 3$]] is the only crystallization path observed. For [Ni(bpy)₃](PF₆)₂, crystals of both structural types can be obtained concomitantly from the same crystallization batch. The γ -phase is systematically twinned by merohedry. The dramatic and unpredictable change in the packing pattern of the very similar building

blocks within this series arises from a delicate balance between the intermolecular forces. Distinct intermolecular interactions with different directionalities can be identified in the two structure types. Through careful analysis of the crystal and molecular structures, a trend with respect to molecular size and shape on going from [Ru(bpy)₃](PF₆)₂ to [Zn(bpy)₃](PF₆)₂ can be established. Even though one might speculate that increasing the size of the molecular cation should destabilize the β -type structure relative to the γ -type, no conclusive rationalization based solely on structural parameters can be given as regards why the relative order of the two local minima on the energy hypersurface should become inverted.

Introduction

Crystal structures of molecular solids are the result of cooperative molecular (chiral) recognition and self-assembly leading to a favourable 3D arrangement. Recognition involves the storage of information at the molecular level and its manifestation at the supramolecular level in a double-complementary fashion, taking into account energetic as well as geometrical requirements.^[2,3] However, the ways in which individual noncovalent forces compete with or reinforce one another in complex systems are poorly understood.

Dunitz^[4,5] succinctly described the crystal as the “*supramolecule par excellence*”. Indeed, each observed packing pattern represents the culmination of highly specific and amazingly precise molecular (chiral) recognition based on noncovalent interactions. Consequently, each crystal structure contains a wealth of valuable information about the ways in which the multitude of noncovalent intermolecular interactions compete and collaborate to achieve their subtle balance.^[6] Careful analysis of crystal structures, packing motifs, and distinct differences in intramolecular geometries should make available the inherent information, thereby assisting in the development of a better understanding of the “*grammar of crystal packing*”.^[7] Besides the more general utility of these rules in the syntheses of designed molecular

materials (i.e. for “crystal engineering”), a practical application might be the development of strategies for increasing the likelihood of conglomerate crystallization.

Conglomerate crystallization is defined as the phenomenon whereby a racemic solution or melt produces a mechanical mixture of enantiomorphic, homochiral crystals, i.e. each individual crystal (or at least domain in the case of racemic twinning) contains a single enantiomer.^[8,9] The phenomenon of conglomerate crystallization can be utilized for optical resolution by the so-called method of “resolution by entrainment”, but it is relatively rare; its frequency has been estimated to be in the range 5–10%.^[10]

Tris(chelate)–metal complexes of planar ligands, [M(L–L)₃]ⁿ⁺ (e.g. L–L: phen = 1,10-phenanthroline, bpy = 2,2′-bipyridine, bpdz = 3,3′-bipyridazine, bpm = 4,4′-bipyrimidine, bpym = 2,2′-bipyrimidine, bpz = 2,2′-bipyrazine) are especially well suited for studying crystal packing phenomena.^[11–13] On the one hand, these propeller-shaped, chiral molecules display a very corrugated molecular form. In Lehn’s^[2] notation, much information is stored at the molecular level, which will inevitably be manifested at the supramolecular level when neighbouring molecular ions interpenetrate to achieve maximum packing density. Moreover, this molecular recognition will not be obscured by gross intramolecular changes since the molecular ions are rather rigid. On the other hand, such molecular systems are extremely flexible. The central atom and its oxidation state may be varied over a wide range and this allows for a fine, systematic tuning of the component parts. Such alterations should help us to gain further insight into

[‡] Part 5: Ref.^[1]

[a] Institut für Anorganische Chemie der Universität Regensburg, 93040 Regensburg, Germany
Fax: (internat.) + 49-(0)941/943-3261
E-mail: josef.breu@chemie.uni-regensburg.de

the relative strengths, directionalities, and structural influences of the various noncovalent forces.

The crystal structures of the true racemate β -[Ru(bpy)₃](PF₆)₂ [14,15] and its closely related low-temperature polymorph α -[Ru(bpy)₃](PF₆)₂ [16] have been known for some time. Of the analogous molecular salts of the first-row transition metals, only the structure of [Fe(bpy)₃](PF₆)₂ has been reported [17] to be isomorphous with that of β -[Ru(bpy)₃](PF₆)₂. All others are absent from the Cambridge Structural Database (CSD), [18] probably because the structures could not be successfully refined. For example, as early as 1983, Ferguson and Herren [19] recognized that in contrast to the Ru analogue, [Zn(bpy)₃](PF₆)₂ undergoes spontaneous resolution upon crystallization. However, they continued: "Attempts to determine the structure by X-ray methods proved fruitless and the difficulties were consistent with perfect multiple twinning." Solution of the crystal structure was claimed in two later publications [20,21] and cell data were given, but the structural details were never published as no satisfactory structure refinement could be accomplished. [22]

After having solved the twinning problem, we are able to report herein the detailed molecular and crystal structures of the enantiomorphic structure type γ -[M(bpy)₃](PF₆)₂ (M = Ni, Zn, Ru) and compare them with those of the true racemate β -[M(bpy)₃](PF₆)₂ (M = Ni, Ru).

Results and Discussion

Braga, Grepioni, and co-workers, who have been at the forefront of developing an organometallic "branch" of crystal engineering, conclude from their experience [23] that "objects of similar shape tend to pack in a similar manner, provided that the type of noncovalent interactions at work are not significantly altered." Contrary to this, we have found that even minor modifications in molecular size and shape induced by variation of the central atom drastically alter the crystallization behaviour of the hexafluorophosphate salts of [M(bpy)₃]²⁺. With M = Fe, Ru, the racemic solutions crystallize as true racemates in the β -type, while for M = Zn the racemic structure could not be obtained, as spontaneous resolution (γ -type) is the only crystallization path observed. Interestingly, for [Ni(bpy)₃](PF₆)₂, crystals of both structure types can be obtained concomitantly [24] from the same crystallization batch. Finally, since [Ru(bpy)₃]²⁺ is inert towards racemization, the γ -type can be "forced" upon [Ru(bpy)₃](PF₆)₂ by chemical resolution prior to crystallization. Enantiomerically pure [Ru(bpy)₃](PF₆)₂ can no longer crystallize in the centrosymmetric β -type, but must crystallize in an enantiomorphic structure with a space group that contains no improper symmetry operations. The dramatic and unpredictable change in the packing arrangement of the very similar building blocks within this series arises from a delicate balance between the intermolecular forces. The following detailed analysis and interpretation of systematic changes in the molecular shapes and intermolecular parameters of the crystal pack-

ings within this series should help to establish trends for these systems and to recover some of the information concerning noncovalent forces encoded in these polymorphic modifications.

Even for these rather rigid units, the geometries observed in the solid state result from the interplay of intra- and intermolecular interactions. To explore the effect of packing forces on the intramolecular geometry, the structure of β -[Ru(bpy)₃](PF₆)₂ was redetermined at a low temperature (200 K) intermediate between those of the prior determinations of the α -type (105 K) [16] and the β -type (294 K). [15]

Finally, the structure of γ -[Ni(bpy)₃](PF₆)₂ was determined twice using two different crystals at the same temperature to get an estimate of the variance in the intermolecular and intramolecular parameters introduced by statistical errors inherent to any structure determination. Not surprisingly, the structural parameters were found to agree within experimental error, but their influence on the packing energies [25] was noticeable.

Comparison of Crystal Structures

Both the β - and γ -type structures are composed of layers of complex cations extending parallel to the *ab* plane, with the anions fully immersed in the layers (Figure 1 and Figure 2). In both structures, the cation layers are homochiral (Figure 3 and Figure 4). However, while in β -[M(bpy)₃](PF₆)₂ layers of complex cations with Λ and Δ configuration alternate along *c*, in the γ -type structure layers of the same chirality are stacked along *c*. The molecular cations are arranged in a hexagonal primitive array in both structures and the distances between the metal atoms in the plane are similar {e.g. 10.3809(7) Å and 10.6453(6) Å in γ - and β -[Ru(bpy)₃](PF₆)₂, respectively; see Table 1}.

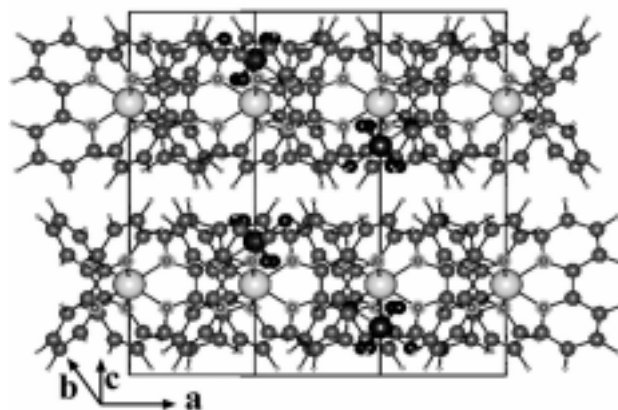
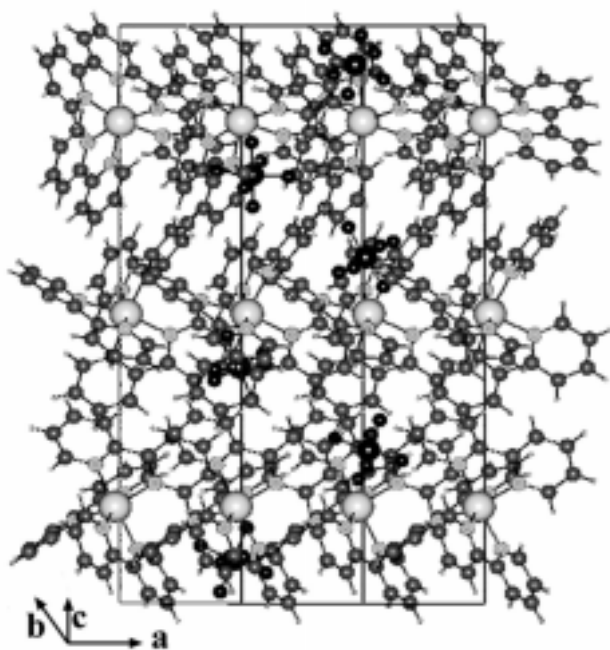
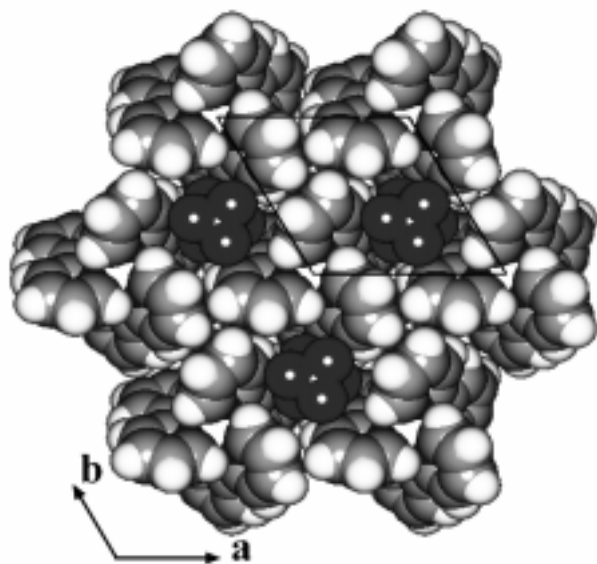
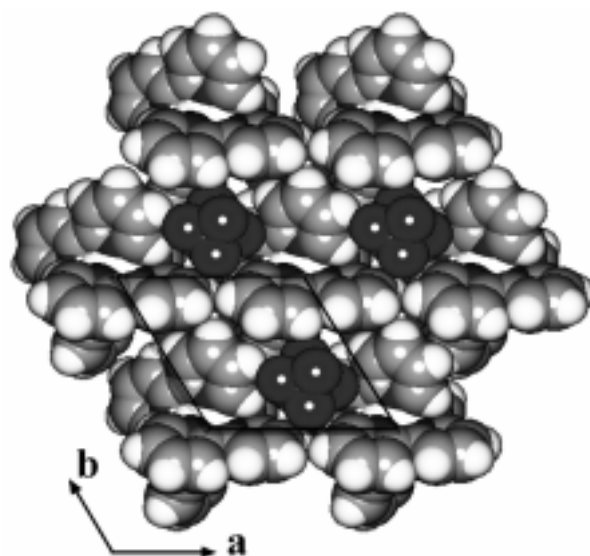


Figure 1. Crystal-packing diagram of β -[M(bpy)₃](PF₆)₂

In the β -phase, the complex cations occupy *D*₃ sites and are oriented with their *C*₃ axes exactly perpendicular to the layers and with their *C*₂ axes extending exactly along the hexagonal axes. In contrast, the cations in the γ -phase are

Figure 2. Crystal-packing diagram of γ -[M(bpy)₃](PF₆)₂Figure 3. Space-filling packing diagram of the complex cation layer in β -[M(bpy)₃](PF₆)₂

effectively “tipped over”. Their pseudo C_3 axes lie approximately in the ab plane. Moreover, the pseudo C_2 axes are not aligned along the hexagonal axes as would be required in the higher symmetry space group $P3_221$ (or $P3_121$), but rather are inclined towards the ab and ac planes (for $\angle C_2|ab, \angle C_2|ac$, see Table 1). The rigorous point symmetry of the cation is C_1 rather than C_2 . Presumably, this slight distortion permits a more efficient packing. Furthermore, this induces a small dipole moment in the unit cell in the c direction, cancelling out of which might, in turn, be the reason for the systematic twinning of this structure type.

Figure 4. Space-filling packing diagram of the complex cation layer in γ -[M(bpy)₃](PF₆)₂

The packing coefficients (Table 1) are similar for both structure types. The absence of improper symmetry elements in the γ -structure does not hamper packing efficiency. This is in line with a study of a larger number of systems, in which no clear trends regarding the densities of true racemates and conglomerates were found either.^[26] Despite the corrugated molecular shape, more than one arrangement of almost equal density is possible.

In neither of these close-packed layers do neighbouring complex cations interpenetrate. Instead, the voids are filled with anions. However, the interlocking of the corrugated van der Waals surfaces in the stacking direction (c) is notable and very distinct for both structure types. In the β -structure, racemic columns of complex cations with colinear C_3 axes extend along c . Along the columns, complexes of opposite chirality are engaged like gearwheels with the tips of the ligands interacting (Figure 5a) and relatively short cation–cation contacts arise {e.g. 8.1494(5) Å for β -[Ru(bpy)₃](PF₆)₂; see Table 1}. This stacking results in a T-shaped geometry of adjacent aromatic ligands.^[27] In the γ -structure, homochiral columns of cations related by the 3₁ (or 3₂) screw axis are observed. The relative orientation of the C_3 axes of neighbouring cations is therefore reasonably close to the tetrahedral angle, which has been recognized as a preferred mutual orientation for an active pair of propeller-shaped molecules based on van der Waals interactions.^[28,29] This mutual arrangement affords two “shifted π -stacks” of adjacent pyridine rings per complex cation (Figure 5c), which are in close contact {8.7601(6) Å for γ -[Ru(bpy)₃](PF₆)₂; see Table 1}. The shortest perpendicular distances between the centroid of one bipyridine ring and the plane of the second ring in the diad are, for instance, 3.689 Å and 3.496 Å in γ -[Ru(bpy)₃](PF₆)₂.

The intermolecular interactions along the cationic chain for both structure types appear to be controlled by so-called “ π – π interactions”.^[30–32] Lateral interactions of this kind are commonly encountered motifs in the crystal packings

Table 1. Selected intermolecular parameters

	[Ru(bpy) ₃](PF ₆) ₂		[Ni(bpy) ₃](PF ₆) ₂		[Zn(bpy) ₃](PF ₆) ₂	
	β_{200}	γ_{200}	β_{240}	$\gamma_{200}(1)$	$\gamma_{200}(2)$	γ_{200}
MM _{column} [Å]	8.1494(5)	8.7601(6)	8.2345(5)	8.7158(9)	8.7136(12)	8.7237(6)
MM _{layer} [Å]	10.6453(6)	10.3809(7)	10.6585(6)	10.3534(11)	10.3599(12)	10.3873(8)
MP [Å]	6.4422(5)	6.248(2)	6.4703(6)	6.183(2)	6.184(2)	6.096(2)
		6.249(2)		6.249(2)	6.251(2)	6.163(2)
		6.389(1)		6.397(1)	6.398(1)	6.362(1)
		6.500(2)		6.541(2)	6.551(2)	6.638(2)
		6.802(2)		6.760(2)	6.764(2)	6.850(2)
		6.845(2)		6.815(2)	6.817(2)	6.902(1)
Cg _{perp.} [Å] ^[a]		3.689/3.496		3.713/3.505	3.712/3.502	3.757/3.493
pack. coeff. ^[b]	0.697	0.685	0.689	0.689	0.690	0.691
< C ₂ <i>ab</i>	0.00	1.78	0.00	1.65	1.41	1.67
< C ₂ <i>ac</i>	0.00	4.95	0.00	4.63	4.58	6.13

^[a] Shortest perpendicular distances between the centroid of one bipyridine ring and the plane of the second ring in the “shifted π -stacks”.

— ^[b] Ref.^[61]

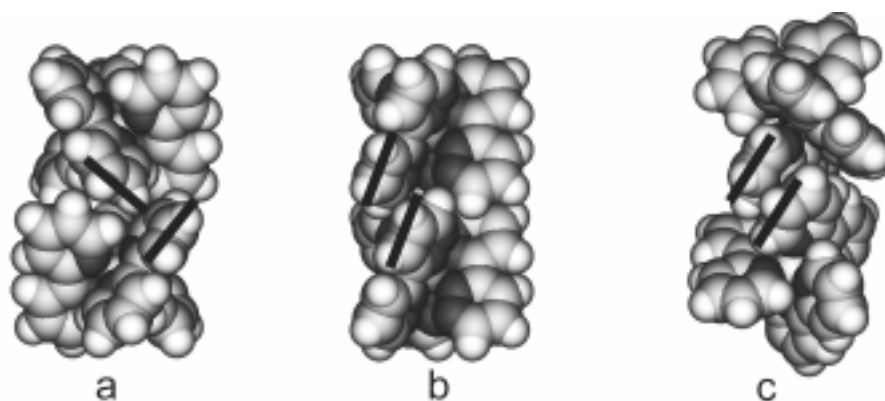


Figure 5. Space-filling packing diagram of the complex cation columns running along *c* in β -[M(bpy)₃](PF₆)₂ (a), [Ni(bpdz)₃](ClO₄)₂ ^[49] (b), and γ -[M(bpy)₃](PF₆)₂ (c) displaying the interlocking of adjacent cations in the various “ π - π interactions”.

of aromatic compounds^[33,34] and their general importance in molecular recognition has been acknowledged.^[35,36] Recent experimental^[35,37–39] and theoretical^[31,40–42] work has shown that both dispersion forces and electrostatic C–H \cdots π interactions contribute towards the favourable “ π - π interactions”. The relative importance of these two contributions is a matter of debate,^[38,39] especially for the T-shaped arrangement. The inherent polarity of aromatic systems stems from the electron-rich core being surrounded by an electron-poor torus of hydrogen atoms. This electrostatic contribution accounts for the energetic preference of both T-shaped and shifted π -stacked arrangements. Which one is preferred depends on the relative magnitude of the dispersion and C–H \cdots π interactions and therefore on the planar extension of the aromatic system. Even for the simplest system, i.e. the benzene dimer in the gas phase, there is an ongoing dispute as to which local minimum on the potential energy hypersurface represents the more stable configuration.^[41,43–47] In the solid state, the two local minima manifest themselves in herringbone and/or π -stacked crystal packing motifs.^[33,34,48] These favourable “ π - π interactions” may facilitate direct cation–cation contacts. However, with [M(L–L)₃]^{*n*+}, the situation is somewhat more complicated than that with simple aromatic systems since the fixing of three aromatic systems in a rigid mutual orientation imposes certain spatial requirements that also de-

pend on the chirality of these complexes. Racemic pairs with colinear C₃ axes, as in β -[Ru(bpy)₃](PF₆)₂, lead to a T-shaped configuration (Figure 5a), for the analogous active pair as observed in [Ni(bpdz)₃](ClO₄)₂ ^[49] a shifted π -stack involving half of a ligand results (Figure 5b), while active pairs with tilted C₃ axes as in the γ -modification yield a shifted π -stack implying a complete ligand.

Despite the spatial restraints imposed by the coordination, “ π - π interactions” are frequently observed in crystal structures of neutral {[Ru(bpy)₃]}^[50] and, more surprisingly, charged propeller-shaped molecules of the type investigated here {[Ru(bpym)₃](PF₆)₂·CH₃CN,^[15] [Ru(phen)₃](PF₆)₂ ^[13]}.

The “coordination” of the cations by anions is quite similar in both the γ - and β -type structures. Each cation is surrounded by six PF₆[–] anions in a trigonal antiprism and the MP distances are all of comparable magnitude (Table 1). This suggests that the monopole–monopole interaction between cations and anions should be very similar in both structural types (see also ref.^[25]).

Grepioni et al.^[23] have shown that for hexafluorophosphate organometallic salts C–H \cdots F interactions play a significant role among the various intermolecular interactions when assisted by the charge difference between anions and cations. In both structure types, we find bonds shorter than the van der Waals cut-off distances (Table 2), these being indicative of specific and directional interactions. However,

Table 2. Hydrogen-bonding geometry [\AA , $^\circ$] for $[\text{Ru}(\text{bpy})_3](\text{PF}_6)_2$

D–H \cdots A ^{[a][b]}	H \cdots A	D \cdots A	D–H \cdots A
β -type:			
C4–H4 \cdots F1 ^[i]	2.4057	3.126(4)	134.21
γ -type:			
C14–H14 \cdots F12 ^[ii]	2.5433	3.153(5)	122.13
C24–H24 \cdots F11 ^[iii]	2.4775	3.236(7)	136.83
C33–H33 \cdots F16	2.4964	3.199(6)	130.77
C35–H35 \cdots F14 ^[iv]	2.4196	3.208(5)	140.35
C36–H36 \cdots F12 ^[iv]	2.4785	3.228(5)	135.72
C45–H45 \cdots F23 ^[v]	2.3073	3.114(11)	142.39
C55–H55 \cdots F22 ^[vi]	2.5350	3.376(11)	147.68
C63–H63 \cdots F23 ^[vii]	2.5414	3.316(13)	138.82

[a] $\text{D}\cdots\text{A} < \text{R}(\text{D}) + \text{R}(\text{A}) + 0.50 \text{ \AA}$, $\text{H}\cdots\text{A} < \text{R}(\text{H}) + \text{R}(\text{A}) - 0.12 \text{ \AA}$, $\text{D–H}\cdots\text{A} > 100.0^\circ$. – [b] Symmetry codes: ^[i] $y, -x + y, -z$. – ^[ii] $1 - y, 1 + x - y, 1/3 + z$. – ^[iii] $-y, x - y, 1/3 + z$. – ^[iv] $x, -1 + y, z$. – ^[v] $x, 1 + y, z$. – ^[vi] $1 - x + y, 1 - x, -1/3 + z$. – ^[vii] $1 - x + y, -x, -1/3 + z$.

it is impossible to even qualitatively assess their relative energetic significance.

The racemic low-temperature polymorph (α -type) represents just a slight distortion of the packing in the β -type^[16,51] and will not be discussed further here.

Comparison of Molecular Structures

The three bpy ligands form a propeller-like trigonal arrangement around the metal atoms. The coordination by the nitrogen atoms is trigonally distorted octahedral owing to the fact that the ligand bite (Figure 6, Table 3) is too short to fit a perfect octahedron. The stereochemistry is completely defined by the normalized bite of the bidentate ligand, $b = \text{N}\cdots\text{N}/\text{M}–\text{N}$, and the angle of twist Θ between the upper and lower triangular faces formed by the N atoms of the bpy ligands (Table 4). The regular octahedron corresponds to $\Theta = 30^\circ$ and $b = 2^{1/2}$. Calculations have shown that distortions from D_3 symmetry are increasingly possible as b is decreased.^[52] The distortions in the γ -phase are indeed quite substantial, as manifested in variations of more than 3° in the $\text{N}–\text{M}–\text{N}$ angles at the base of the trigonal

antiprisms (v, Figure 6). Moreover, the trigonal faces are no longer parallel and the central atoms are displaced from the midpoint between them (Table 4). Apparently, the coordination sphere is rather flexible and can be adjusted within certain limits to suit packing requirements.

Not even the ligands can be treated as rigid units. Admittedly, the bond lengths and bond angles within the pyridine moieties are consistent within experimental error in the different phases and compounds; the rings are planar, and the maximum deviations from the best planes are smaller than 0.03 \AA (Δ_{max} in Table 3). However, the two pyridine rings within a ligand are deflected downwards around the midpoint of the $\text{py}–\text{py}$ bond. This kink can be quantified by the difference between A and B (Table 3), which decreases on going from $[\text{Ru}(\text{bpy})_3](\text{PF}_6)_2$ to $[\text{Zn}(\text{bpy})_3](\text{PF}_6)_2$ while the ligand bite and $\text{M}–\text{N}$ distance increase accordingly. This trend reflects the size of the central cation. The extent of the kink together with the trigonal twist determines the height of the complex cation along the C_3 axis. The smaller the kink and the trigonal twist, the “taller” the complex

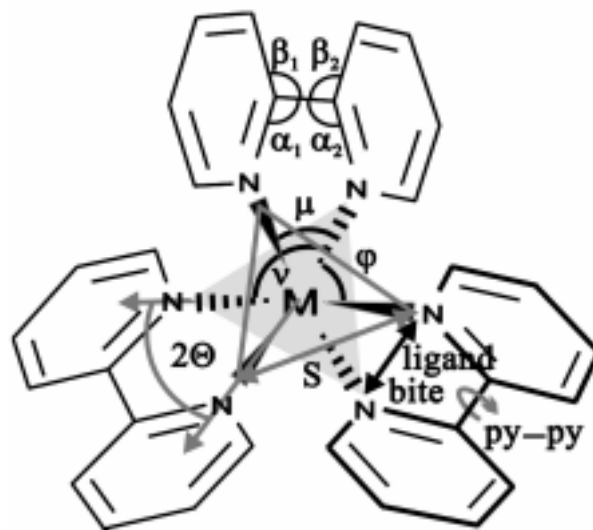


Figure 6. Labelling scheme of the geometrical parameters listed in Tables 3 and 4

Table 3. Selected geometrical data, ligands

	$[\text{Ru}(\text{bpy})_3](\text{PF}_6)_2$			$[\text{Ni}(\text{bpy})_3](\text{PF}_6)_2$			$[\text{Zn}(\text{bpy})_3](\text{PF}_6)_2$
	$\beta_{294}^{[a]}$	β_{200}	γ_{200}	β_{240}	$\gamma_{200}(1)$	$\gamma_{200}(2)$	γ_{200}
ligand bite [\AA] ^[b]	2.607(3)	2.598(3)	2.631(5) 2.612(5) 2.627(5)	2.628(3)	2.653(5) 2.644(4) 2.645(5)	2.641(5) 2.632(5) 2.636(5)	2.678(5) 2.677(4) 2.676(4)
$\text{py}–\text{py}$ [$^\circ$] ^[b]	7.90(19) ^[c]	8.81(13)	12.7(2) 6.7(2) 9.4(3)	8.37(15)	16.2(2) 12.9(2) 10.6(3)	16.3(3) 13.1(2) 10.9(3)	17.2(2) 17.1(1) 8.9(3)
$A = \alpha_1 + \alpha_2$ [$^\circ$] ^[b]	229.4(6)	228.9(4)	230.0(7) 229.4(8) 230.7(7)	230.5(4)	230.8(7) 231.1(8) 231.7(8)	229.8(8) 230.2(8) 231.6(8)	232.3(7) 232.4(8) 233.3(6)
$B = \beta_1 + \beta_2$ [$^\circ$] ^[b]	249.2(6)	247.9(4)	246.4(8) 247.7(8) 246.3(8)	246.4(4)	244.7(8) 245.9(8) 245.9(8)	244.0(9) 246.5(9) 246.0(9)	244.3(8) 244.2(8) 245.7(8)
Δ_{max} [\AA] ^[d]	0.015(2)	0.019(2)	0.028(4)	0.017(2)	0.020(4)	0.026(5)	0.017(4)

[a] For labelling scheme, see Figure 6. – [b] Ref.^[15] – [c] Value given in ref.^[15] is erroneous. – [d] Maximum deviation from the best plane within a single pyridine ring.

Table 4. Selected geometrical data, coordination sphere

	[Ru(bpy) ₃](PF ₆) ₂			[Ni(bpy) ₃](PF ₆) ₂			[Zn(bpy) ₃](PF ₆) ₂
	β ₂₉₄	β ₂₀₀	γ ₂₀₀	β ₂₄₀	γ ₂₀₀₍₁₎	γ ₂₀₀₍₂₎	γ ₂₀₀
M–N [Å]	2.056(2)	2.048(2)	2.058(4) 2.065(3) 2.066(4) 2.067(4) 2.062(3) 2.063(4)	2.067(2)	2.074(4) 2.088(3) 2.072(3) 2.093(3) 2.080(3) 2.093(4)	2.070(4) 2.083(3) 2.076(4) 2.084(4) 2.075(4) 2.085(4)	2.150(4) 2.158(3) 2.147(3) 2.182(3) 2.156(3) 2.182(4)
site symmetry	D ₃	D ₃	C ₁	D ₃	C ₁	C ₁	C ₁
ligand bite	78.67(8)	78.74(8)	79.29(12) 78.41(15) 79.14(12) 92.12(16) 91.40(12) 89.36(13)	78.93(9)	79.21(13) 78.82(12) 78.68(13) 92.53(14) 93.04(12) 91.27(13)	78.96(13) 78.50(16) 78.64(14) 92.43(16) 93.09(14) 91.22(15)	78.86(12) 76.41(11) 76.15(11) 94.80(14) 95.92(11) 93.13(12)
angle, μ [°] ^[a]	89.13(10)	89.51(9)	94.78(15) 95.43(13) 96.75(13) 93.43(12) 94.95(16) 96.59(12)	90.6(1)	93.97(13) 94.72(13) 95.83(13) 92.73(12) 95.10(13) 96.14(12)	94.17(15) 94.86(15) 95.99(14) 92.84(13) 95.34(16) 96.04(15)	93.79(13) 96.10(12) 95.78(12) 92.65(12) 95.97(13) 96.19(11)
ν [°] ^[a]	96.29(9)	96.08(9)	1.271(4) ^[c] 50.5(2) ^[c]	95.49(9)	1.271(3) ^[c] 50.8(1) ^[c]	1.268(5) ^[c] 49.2(2) ^[c]	1.238(4) ^[c] 45.5(2) ^[c]
h ^[b]	1.268(3)	1.269(2)	1.074(2)	1.271(3) ^[c]	1.279(5) ^[c]	1.268(5) ^[c]	1.238(4) ^[c]
2Θ [°] ^[d]	51.9(1)	51.6(1)	1.074(2)	50.8(1) ^[c]	49.3(2) ^[c]	49.2(2) ^[c]	45.5(2) ^[c]
M–t1 [Å] ^[e]	1.049(2)	1.050(4)	1.068(4)	1.074(2)	1.094(3)	1.089(4)	1.126(3)
M–t2 [Å] ^[e]	1.049(2)	1.050(2)	1.082(4)	1.074(2)	1.104(3)	1.098(4)	1.139(3)
t1–M–t2 [°]	180.00	180.00	179.3(2)	180.00	179.2(3)	179.4(3)	179.4(2)
S [Å] ^[f]	3.063(4)	3.046(3)	3.050 ^[b]	3.060(4)	3.066 ^[b]	3.062 ^[b]	3.191 ^[b]

^[a] For labelling scheme, see Figure 6. – ^[b] Normalized ligand bite. – ^[c] Averaged in D₃ symmetry. – ^[d] Trigonal twist. – ^[e] Distances between the central atom and the centre of gravity of the trigonal faces formed by the N atoms of the bpy ligands. – ^[f] Edge length of the base of the trigonal antiprism.

cation. Thus, [Ru(bpy)₃](PF₆)₂ is shorter than [Zn(bpy)₃](PF₆)₂, as indicated by the height of the trigonal antiprisms formed by the N atoms of the bpy ligands (2.100 Å and 2.265 Å, respectively).

The widths of the molecular cations, i.e. their extensions perpendicular to the C₃ axis, are largely determined by the M–N distance since the ligands are pushed further away as the bond lengths increase. The mean lengths of the edges of the bases of the trigonal faces (S, Table 4) increase from 3.046 Å to 3.191 Å on going from [Ru(bpy)₃](PF₆)₂ to [Zn(bpy)₃](PF₆)₂. This suggests that the height/width ratio changes slightly in the series, with [Zn(bpy)₃](PF₆)₂ being relatively larger around the “waist”.

Another intramolecular low-energy mode that the cation takes advantage of to adjust to the local packing environment is the torsion about the py–py bond. Lowering the temperature from 294 K to 200 K, thereby shortening the intermolecular distances, results in an increase in the dihedral angle between the two pyridine rings in the ligand from 7.90(19)° to 8.81(13)° for β-[Ru(bpy)₃](PF₆)₂ (Table 3) and still further to 9.0(4)–10.3(3)° for α-[Ru(bpy)₃](PF₆)₂.^[16] The variation in the γ-phase [6.7(2)–12.7(2)°] is even more notable.

Conclusion

In the realm of organic and organometallic compounds, polymorphism has often been associated with torsional degrees of freedom of molecular fragments bound by single bonds, thus making it conformational in nature. Although

the system under consideration here utilizes its very limited intramolecular degrees of freedom to optimize packing, the molecular shape of the building blocks is to a first approximation the same. A similar example of a rather rigid coordination compound crystallizing in different polymorphs has been recently found in the case of [Pd(dmpz)₂(Hdmpz)₂]₂ (Hdmpz = 3,5-dimethylpyrazole).^[53]

The simple fact that there are coexisting polymorphs in the case of [Ni(bpy)₃](PF₆)₂ emphasizes the importance of kinetic aspects, but it is nevertheless expected that the non-occurrence of γ-[Fe(bpy)₃](PF₆)₂, γ-[Ru(bpy)₃](PF₆)₂, or β-[Zn(bpy)₃](PF₆)₂ on crystallization from the respective racemic solutions can be attributed to thermodynamic factors. At least it is hard to imagine that nucleation kinetics could be so different for these similar systems. On the one hand, careful analysis of the crystal and molecular structures has established a trend with respect to molecular size and shape (Table 4) on going from [Ru(bpy)₃](PF₆)₂ to [Zn(bpy)₃](PF₆)₂. On the other hand, distinct intermolecular interactions with different directionalities (T-shaped as opposed to shifted π-stack π–π interactions) have been identified in the two structure types. However, this gives no indication of their relative strengths, and no rationalization can be given as to why the relative order of the two local minima on the energy hypersurface becomes inverted. This requires an analysis of the packing energies, which will be dealt with in a separate paper.^[25] Given the molecular structure, little can be said a priori on the likelihood of spontaneous resolution of racemic solutions upon crystallization, even though one might speculate that increasing the size of

the molecular cation should destabilize the β -type relative to the γ -type structure. However, size alone cannot give a satisfactory explanation since $[\text{Ru}(\text{bpy})_3](\text{PF}_6)_2$ and $[\text{Ni}(\text{bpy})_3](\text{PF}_6)_2$ are very similar in that respect and yet still display different crystallization behaviour. Evidently, other information at the molecular level, as for instance the molecular electrostatic potential, is also important.

Certainly, the presented case gives a striking example of the sensitivity of crystal packings to even tiny variations in molecular structure. Moreover, the shape of molecular building blocks alone surely does not determine the crystal structure, but rather it is the subtle balance between all the various intermolecular forces. This equilibrium balance of forces embraces many intermolecular interactions; “ π – π interactions” are apparent in crystal structures of $[\text{M}(\text{bpy})_3](\text{PF}_6)_2$ compounds. However, T-shaped and shifted π -stack arrangements compete. Unquestionably, postulation of dominance by a T-shaped arrangement, as in a report by Dance,^[27] is not justified. Moreover, solely on the basis of topology, nothing can be said about the relative contributions of dispersion/repulsion forces and electrostatic C–H $\cdots\pi$ interactions to these “ π – π interactions”.

Experimental Section

Synthesis: All $[\text{M}(\text{bpy})_3](\text{PF}_6)_2$ salts were obtained by metathesis of the corresponding chloride, sulfate, or bromide salts, in turn prepared according to literature procedures.^[54,55] – Optical resolution

of $[\text{Ru}(\text{bpy})_3]^{2+}$, which did not occur spontaneously, was achieved by a modification of the procedure of Dwyer and Gyarfas using potassium antimonyl tartrate.^[56] – Concomitant crystallization of β - and γ - $[\text{Ni}(\text{bpy})_3](\text{PF}_6)_2$ could be achieved by slow evaporation of the solvents from an acetone/water (2:1) solution at ambient temperature. β - $[\text{Ru}(\text{bpy})_3](\text{PF}_6)_2$ could be crystallized from the same solvent mixture, but from ethanol/water (2:1) more suitable single crystals were obtained. The best crystals of γ - $[\text{Ru}(\text{bpy})_3](\text{PF}_6)_2$ and γ - $[\text{Zn}(\text{bpy})_3](\text{PF}_6)_2$ were obtained by recrystallization from acetone/ethanol (5:1).

Crystal Structure Analyses: Relevant crystallographic data and details of the data collection and structure refinement are listed in Table 5. Structure solution and refinement of the β -type structures was straightforward.

All compounds crystallizing in the γ -phase are affected by systematic twinning due to merohedry. This is indicated by a gritty appearance of the crystal faces. The twin antisymmetry space group is $P3_22'1$ (or $P3_12'1$).^[57] Structure solution in this space group proved impossible. In $P3_1$ (and its enantiomorphic space group $P3_2$), direct methods yielded a partial structure model, which could be completed by successive difference Fourier syntheses. However, anisotropic refinement was not feasible until the correct twinning law ([110]) was introduced. The absolute structure was assigned on the basis of the Flack x parameter,^[58] where x is the fractional contribution of the inverted component of a “racemic twin”. It is expected to be zero for the correct structure, unity for the inverted structure, and somewhere in between if racemic twinning is present. For the chemically resolved γ - $[\text{Ru}(\text{bpy})_3](\text{PF}_6)_2$, the assignment is in agreement with the observed specific rotation. Surprisingly, while for γ - $[\text{Zn}(\text{bpy})_3](\text{PF}_6)_2$ each singular crystal seems to be homochiral, for γ - $[\text{Ni}(\text{bpy})_3](\text{PF}_6)_2$ general and racemic twinning has to be refined simultaneously.

Table 5. Crystallographic data and details of the structure determination

	$[\text{Ru}(\text{bpy})_3](\text{PF}_6)_2$ β_{200}	γ_{200}	$[\text{Ni}(\text{bpy})_3](\text{PF}_6)_2$ β_{240}	$\gamma_{200}(1)$	$\gamma_{200}(2)$	$[\text{Zn}(\text{bpy})_3](\text{PF}_6)_2$ γ_{200}
Empirical formula	$\text{C}_{30}\text{H}_{24}\text{RuN}_6\cdot 2(\text{F}_6\text{P})$	$\text{C}_{30}\text{H}_{24}\text{RuN}_6\cdot 2(\text{F}_6\text{P})$	$\text{C}_{30}\text{H}_{24}\text{NiN}_6\cdot 2(\text{F}_6\text{P})$	$\text{C}_{30}\text{H}_{24}\text{NiN}_6\cdot 2(\text{F}_6\text{P})$	$\text{C}_{30}\text{H}_{24}\text{NiN}_6\cdot 2(\text{F}_6\text{P})$	$\text{C}_{30}\text{H}_{24}\text{NiN}_6\cdot 2(\text{F}_6\text{P})$
Molecular mass	859.56	859.56	817.18	817.18	817.18	823.88
Crystal system	trigonal	trigonal	trigonal	trigonal	trigonal	trigonal
Space group	$P3_1$ (No. 165)	$P3_1$ (No. 144)	$P3_1$ (No. 165)	$P3_1$ (No. 144)	$P3_1$ (No. 144)	$P3_1$ (No. 144)
a [Å]	10.6453(5)	10.3809(4)	10.6585(6)	10.3534(4)	10.3599(5)	10.3873(5)
c [Å]	16.2987(9)	26.2576(13)	16.4690(10)	26.1231(14)	26.1163(13)	26.1309(16)
V [Å ³]	1599.56(14)	2450.51(18)	1620.28(16)	2425.05(19)	2427.5(2)	2441.7(2)
Z	2	3	2	3	3	3
D_x [g/cm ³]	1.785	1.747	1.675	1.679	1.677	1.681
$F(000)$	856	1284	824	1236	1236	1242
μ [cm ^{−1}]	6.9	6.8	8.0	8.0	8.0	9.6
Crystal size [mm]	$0.40 \times 0.18 \times 0.18$	$0.52 \times 0.30 \times 0.24$	$0.70 \times 0.26 \times 0.26$	$0.50 \times 0.18 \times 0.17$	$0.30 \times 0.16 \times 0.15$	$0.48 \times 0.30 \times 0.30$
Crystal shape	hexagonal prism	hexagonal needle	hexagonal prism	hexagonal needle	hexagonal needle	hexagonal needle
Crystal colour	dark orange	dark orange	light brown	light red	light red	colourless
Temperature [K]	200	200	240	200	200	200
Radiation [Å]	Mo- K_α 0.71069	Mo- K_α 0.71069	Mo- K_α 0.71069	Mo- K_α 0.71069	Mo- K_α 0.71069	Mo- K_α 0.71069
θ range [°]	2.2–25.6	2.4–25.2	2.4–25.5	2.4–25.6	2.3–25.6	2.4–25.6
h	−11/12	−12/10	−12/12	−12/12	−12/12	−12/12
k	−12/11	−10/12	−12/11	−11/5	−12/12	−12/12
l	−19/19	−31/31	−16/19	−27/30	−28/27	−24/31
Tot. no. of reflections	7163	10150	5510	8836	12038	10839
Unique reflections	1006	5669	996	5317	5700	5317
R_{int}	0.034	0.022	0.026	0.019	0.028	0.021
Observed reflections	820 [$I_o > 2\sigma(I_o)$]	5645 [$I_o > 2\sigma(I_o)$]	844 [$I_o > 2\sigma(I_o)$]	5172 [$I_o > 2\sigma(I_o)$]	5253 [$I_o > 2\sigma(I_o)$]	5248 [$I_o > 2\sigma(I_o)$]
Refined parameters	78	461	78	463	463	461
$R1^{[a]}$	0.0261	0.0242	0.0415	0.0278	0.0311	0.0261
$wR2^{[a][b]}$	0.0668	0.0622	0.1260	0.0682	0.0608	0.0690
$S^{[c]}$	0.98	1.03	1.07	1.02	0.95	1.04
d , $e^{[d]}$	0.0495, 0.0	0.0528, 0.0597	0.0844, 0.5662	0.0494, 0.0	0.0315, 0.0	0.0569, 0.0
Flack x parameter ^[e]	—	−0.01(3)	—	0.505(9)	0.520(9)	0.00(1)
$\Delta\rho_{\text{min}}$, $\Delta\rho_{\text{max}}$ [e [−] /Å ³]	−0.39, 0.37	−0.35, 0.44	−0.40, 0.47	−0.22, 0.35	−0.20, 0.28	−0.22, 0.31

^[a] $R1 = \Sigma ||F_o| - |F_c|| / \Sigma |F_o|$. – ^[b] $wR2 = \{\Sigma [w(F_o^2 - F_c^2)^2] / \Sigma [w(F_o^2)^2]\}^{1/2}$. – ^[c] $S = \{\Sigma [w(F_o^2 - F_c^2)^2] / (n - p)\}^{1/2}$, where n = no. of refl. and p = total no. of parameters refined. – ^[d] $w = 1/[\sigma^2(F_o^2) + (dP)^2 + eP]$, where $P = [2F_c^2 + \text{Max}(F_o^2, 0)]/3$. – ^[e] Ref.^[58]

All structures were refined in a consistent manner employing the SHELX-97 program package.^[59] SHELX refines against F^2 and all data were used in the full-matrix least-squares refinement. H atoms were placed in idealized positions and were refined with fixed isotropic displacement parameters of $1.2U_{eq}$ (parent C). All other atoms were refined anisotropically. The weighting scheme recommended by the program was used and refinement was continued until complete convergence (maximum shift/esd < 0.001) was achieved. Graphics and geometrical parameters were generated using the PLATON package.^[60]

Crystallographic data (excluding structure factors) for the structures reported in this paper have been deposited with the Cambridge Crystallographic Data Centre as supplementary publication nos. CCDC-101675 $\{\beta_{200}[\text{Ru}(\text{bpy})_3](\text{PF}_6)_2\}$, -101676 $\{\gamma_{200}[\text{Ru}(\text{bpy})_3](\text{PF}_6)_2\}$, -101677 $\{\beta_{240}[\text{Ni}(\text{bpy})_3](\text{PF}_6)_2\}$, -101678 $\{\gamma_{200}(1)-[\text{Ni}(\text{bpy})_3](\text{PF}_6)_2\}$, -101679 $\{\gamma_{200}(2)-[\text{Ni}(\text{bpy})_3](\text{PF}_6)_2\}$, and -101680 $\{\gamma_{200}[\text{Zn}(\text{bpy})_3](\text{PF}_6)_2\}$. Copies of the data can be obtained free of charge on application to the CCDC, 12 Union Road, Cambridge CB2 1EZ, U.K. [Fax: (internat.) + 44-1223/336-033; E-mail: deposit@ccdc.cam.ac.uk].

Since submission of the manuscript we have been informed that the structure of γ - $[\text{Zn}(\text{bpy})_3](\text{PF}_6)_2$ has meanwhile also been solved by Bernal's group; the manuscript will soon be submitted to *J. Chem. Soc., Dalton Trans.*^[62]

Acknowledgments

We would like to thank Prof. Dr. K.-J. Range for making equipment available and for support in various areas, the Fonds der Chemischen Industrie, and the DFG for financial support. Furthermore, we thank the Degussa AG for a donation of $\text{RuCl}_3 \cdot 3\text{H}_2\text{O}$.

- [1] J. Breu, N. Raj, C. R. A. Catlow, *J. Chem. Soc., Dalton Trans.* **1999**, 835–845.
- [2] J. M. Lehn, *Pure Appl. Chem.* **1994**, 66, 1961–1966.
- [3] J. M. Lehn, in *Lock-and-Key Principle* (Ed.: J. P. Behr), John Wiley & Sons Ltd., **1994**.
- [4] J. D. Dunitz, *Acta Crystallogr. B* **1995**, 51, 619–631.
- [5] J. D. Dunitz, in *The Crystal as a Supramolecular Entity* (Ed.: G. R. Desiraju), John Wiley & Sons Ltd., **1996**.
- [6] C. B. Aakeröy, *Acta Crystallogr. B* **1997**, 53, 569–586.
- [7] C. P. Brock, J. D. Dunitz, *Chem. Mater.* **1994**, 6, 1118–1127.
- [8] I. Bernal, J. Cetrullo, J. Myrczek, J. W. Cai, W. T. Jordan, *J. Chem. Soc., Dalton Trans.* **1993**, 1771–1776.
- [9] Z. Bocskei, D. Kozma, K. Simon, E. Fogassy, *J. Chem. Res. (S)* **1995**, 160–161.
- [10] J. Jacques, A. Collet, S. H. Wilen, *Enantiomers, Racemates, and Resolution*, John Wiley & Sons, New York, **1981**.
- [11] H. Lai, D. S. Jones, D. C. Schwind, D. P. Rillema, *J. Crystallogr. Spectrosc. Res.* **1990**, 20, 321–325.
- [12] J. Breu, P. Belser, H. Yersin, *Acta Crystallogr. C* **1996**, 52, 858–861.
- [13] J. Breu, A. J. Stoll, *Acta Crystallogr. C* **1996**, 52, 1174–1177.
- [14] D. P. Rillema, D. J. Jones, *J. Chem. Soc., Chem. Commun.* **1979**, 849–851.
- [15] D. P. Rillema, D. S. Jones, C. Woods, H. A. Levy, *Inorg. Chem.* **1992**, 31, 2935–2938.
- [16] M. Biner, H.-B. Bürgi, A. Ludi, C. Rohr, *J. Am. Chem. Soc.* **1992**, 114, 5197–5203.
- [17] S. Dick, *Z. Kristallogr. New Cryst. Struct.* **1998**, 213, 356.
- [18] F. H. Allen, O. Kennard, *Chem. Des. Autom. News* **1993**, 8, 31–37.
- [19] J. Ferguson, F. Herren, *Chem. Phys.* **1983**, 76, 45–59.
- [20] J. Ferguson, E. Krausz, *Inorg. Chem.* **1987**, 26, 1383–1386.
- [21] E. Krausz, G. Moran, *J. Luminesc.* **1988**, 42, 21–27.
- [22] I. Bernal, private communication, **1994**.
- [23] F. Grepioni, G. Cojazzi, S. M. Draper, N. Scully, D. Braga, *Organometallics* **1998**, 17, 296–307.
- [24] J. Bernstein, R. J. Davey, J.-O. Henck, *Angew. Chem.* **1999**, 111, 3646–3669; *Angew. Chem. Int. Ed.* **1999**, 38, 3440–3461.
- [25] J. Breu, H. Domel, *Eur. J. Inorg. Chem.* **2000**, 2409–2419, subsequent paper.
- [26] C. P. Brock, W. B. Schweizer, J. D. Dunitz, *J. Am. Chem. Soc.* **1991**, 113, 9811–9820.
- [27] I. Dance, M. Scudder, *J. Chem. Soc., Dalton Trans.* **1998**, 1341–1350.
- [28] R. Kuroda, S. F. Mason, C. D. Rodger, R. H. Seal, *Mol. Phys.* **1981**, 42, 33–50.
- [29] R. Kuroda, P. Biscarini, *Mol. Cryst. Liq. Cryst. Sci. Tech. A* **1996**, 278, A275–A284.
- [30] T. Liljefors, I. Petterssen, *J. Comput. Chem.* **1987**, 8, 1139–1145.
- [31] W. L. Jorgensen, D. L. Severance, *J. Am. Chem. Soc.* **1990**, 112, 4768–4774.
- [32] C. A. Hunter, in *From Simplicity to Complexity in Chemistry – and Beyond* (Ed.: A. Müller), Vieweg, Braunschweig, **1996**.
- [33] G. R. Desiraju, A. Gavezzotti, *Acta Crystallogr. B* **1989**, 45, 473–482.
- [34] J. D. Dunitz, A. Gavezzotti, *Acc. Chem. Res.* **1999**, 32, 677–684.
- [35] C. A. Hunter, *Angew. Chem.* **1993**, 105, 1653–1655; *Angew. Chem. Int. Ed.* **1993**, 32, 1584–1586.
- [36] C. A. Hunter, *Phil. Trans. R. Soc. London, A* **1993**, 345, 77–85.
- [37] H. Adams, K. D. M. Harris, G. A. Hembury, C. A. Hunter, D. Livingstone, J. F. McCabe, *Chem. Commun.* **1996**, 2531–2532.
- [38] C. S. Wilcox, E. Kim, S. Paliwal, *J. Am. Chem. Soc.* **1998**, 120, 11192–11193.
- [39] C. S. Wilcox, S. Paliwal, S. Geib, *J. Am. Chem. Soc.* **1994**, 116, 4497–4498.
- [40] G. Karlström, P. Linse, A. Wallqvist, B. Jönsson, *J. Am. Chem. Soc.* **1983**, 105, 3777–3782.
- [41] P. Hobza, H. L. Selzle, E. W. Schlag, *J. Phys. Chem.* **1996**, 100, 18790–18794.
- [42] P. Hobza, V. Spirko, H. L. Selzle, E. W. Schlag, *J. Phys. Chem. A* **1998**, 102, 2501–2504.
- [43] P. Hobza, H. L. Selzle, E. W. Schlag, *J. Phys. Chem.* **1993**, 97, 3937–3938.
- [44] W. Scherzer, O. Kratzschmar, H. L. Selzle, E. W. Schlag, *Z. Naturforsch., A* **1992**, 47, 1248–1252.
- [45] V. A. Venturo, P. M. Felker, *J. Chem. Phys.* **1993**, 99, 748–751.
- [46] E. Arunan, H. S. Gutowsky, *J. Chem. Phys.* **1993**, 98, 4294–4296.
- [47] J. A. Niesse, H. R. Mayne, *J. Phys. Chem.* **1997**, 101, 9137–9137.
- [48] A. Gavezzotti, *Chem. Phys. Lett.* **1989**, 161, 67–72.
- [49] D. Onggo, A. D. Rae, H. A. Goodwin, *Inorg. Chim. Acta* **1990**, 178, 151–163.
- [50] E. Perez-Cordero, C. Campana, L. Echegoyen, *Angew. Chem.* **1997**, 109, 85–88; *Angew. Chem. Int. Ed. Engl.* **1997**, 36, 137–140.
- [51] J. Breu, C. Kratzer, H. Yersin, *J. Am. Chem. Soc.*, in print.
- [52] D. L. Kepert, *Inorganic Chemistry*, Springer Verlag, Berlin, **1982**.
- [53] N. Masciocchi, G. A. Ardizzoia, G. La Monica, M. Moret, A. Sironi, *Inorg. Chem.* **1997**, 36, 449–454.
- [54] F. M. Jaeger, J. A. van Dijk, *Z. Anorg. Allg. Chem.* **1936**, 227, 273–327.
- [55] M. M. T. Khan, R. C. Bhardwaj, C. Bhardwaj, *Polyhedron* **1990**, 9, 1243–1248.
- [56] V. Joshi, P. K. Ghosh, *J. Am. Chem. Soc.* **1989**, 111, 5604–5612.
- [57] T. Araki, *Z. Kristallogr.* **1991**, 194, 161–191.
- [58] H. D. Flack, *Acta Crystallogr. A* **1983**, 39, 876–881.
- [59] G. M. Sheldrick, *SHELX-97*, University of Göttingen, **1997**.
- [60] A. L. Spek, *Acta Crystallogr. A* **1990**, 46, C34.
- [61] A. I. Kitajgorodski, *Molecular Crystals and Molecules*, Academic Press, New York, **1973**.
- [62] I. Bernal, private communication, **2000**.

Received February 8, 2000

[I00042]